Case Studies in Mechanical Systems and Signal Processing 3 (2016) 28–33

Contents lists available at ScienceDirect

Case Studies in Mechanical Systems and Signal Processing

journal homepage: www.elsevier.com/locate/csmssp

Short communication

Upgrade of an automated line for plastic cap manufacture based on experimental vibration analysis

Alberto Martini*, Marco Troncossi

DIN—Department of Engineering for Industry, University of Bologna, Viale del Risorgimento 2, 40136 Bologna (BO), Italy

ARTICLE INFO

Article history:
Received 5 January 2016
Received in revised form 18 March 2016
Accepted 18 March 2016
Available online 19 March 2016

Keywords:
Vibration monitoring
Experimental analysis
Non-contact measurement

ABSTRACT

The study deals with an experimental campaign to analyze the effects on an automatic machine for plastic cap assembly of the increased vibrations occurring when speeding up its operation. The new velocity specifications are required by the machine manufacturer for raising the production capacity. The analysis successfully identified the functional units critically affected by elastodynamic issues related to the speed increment. Hence it permitted to focus the redesign process on the critical groups in order to implement the desired machine upgrade by means of limited modifications to the current machine version. The most relevant experimental results are presented and discussed. The paper also reports data provided by further tests carried out on a machine variant (obtained after the implementation of the first design modifications), which prove the effectiveness of the proposed solutions to improve the machine performance.

1. Introduction

The presented activity relates to the upgrade of an automated line for the manufacture of plastic resealable opening devices for packages of pourable food [1]. The primary objective is increasing the machinery nominal production capacity by about 50%, from 680 to 1000 products per minute (*ppm*). This goal has to be achieved through a proper rise in the working velocity and only limited modifications of the existing machinery design.

This study focuses on the automatic machine that assembles the end product starting from its three components. The remarkable speed increment required to meet the desired production target may trigger elastodynamic phenomena possibly detrimental for both the performance and the reliability of the machine. An experimental campaign was carried out to investigate these potential issues by means of vibration measurements. The analysis aimed at identifying the functional groups characterized by critical elastodynamic behavior, thus providing the guidelines for a partial machine redesign.

The current configuration does not allow exceeding 25% of the nominal production capacity. Hence, the experiments were designed both to monitor (when possible) and to predict the machine behavior when operating in different working conditions, by arranging special sensor and machine setup.

The analysis yielded a reliable estimation of the machine elastodynamic behavior, thus permitting to define the required design modifications. Relevant results concerning some critical functional units are presented and discussed. Measurements from follow-up tests performed after implementing some modifications of the most critical unit confirmed a significant enhancement of the machine performance.

* Corresponding author at: Via Fontanelle 40, 47121 Forlì (FC), Italy.
E-mail address: alberto.martini6@unibo.it (A. Martini).

http://dx.doi.org/10.1016/j.csmssp.2016.03.002
2351-9886/

2. Description of the assembly machine

A simplified schematic of the machine layout is presented in Fig. 1, where only the main functional units are shown. The machine reference coordinate system is also reported. A pick-and-place unit (referred to as *P&P1*) takes the three product components (*Comps*) from the corresponding buffers, located next to the machine input area (*IN*), and loads them onto properly shaped trays. Each product tray carries 10 items of each *Comp*, so that 10 caps are assembled in a working cycle. The trays are conveyed by the *Main Transfer Unit* (*MTU*), with intermittent motion, to the next functional groups, for subsequent operations (performed during the rest phase of the *MTU* cycle). The *MTU* is driven by a power transmission chain formed by an *Indexer* and a *Timing Belt* (*TB*). The *Orientation unit* (*OR*) rotates the *Comps* around the vertical axis (direction *Z*) to provide them with the required relative orientations. The assembly task is performed in two steps by the two *Assembly units* (denoted as *As1* and *As2*, respectively). A second pick-and-place unit (*P&P2*), mechanically coupled to the *P&P1* by the *Linkage*, transfers the assembled caps from the trays to the end product buffer, located at the machine output area (*OUT*). The unit referred to as *Lock* engages the product trays processed by the functional units to ensure their accurate positioning during the related operations.

3. Experimental setup and test conditions

Since very few information about the elastodynamic behavior of the machine was available, all the main units and structures were monitored by proper transducers. Preliminary visual inspection of working cycles at 840 *ppm* had reveled significant oscillations affecting both the *Linkage* and the *MTU*, which therefore underwent deeper investigations. In particular, the displacement and the velocity of the product trays along the conveying direction (*Y*-axis) were detected by a laser vibrometer (Polytec HSV-2002, Fig. 2a). These measurements required arranging two “dummy trays” that were installed on the *MTU* by replacing two adjacent product trays. Both dummy trays feature a reflective surface targeted by the

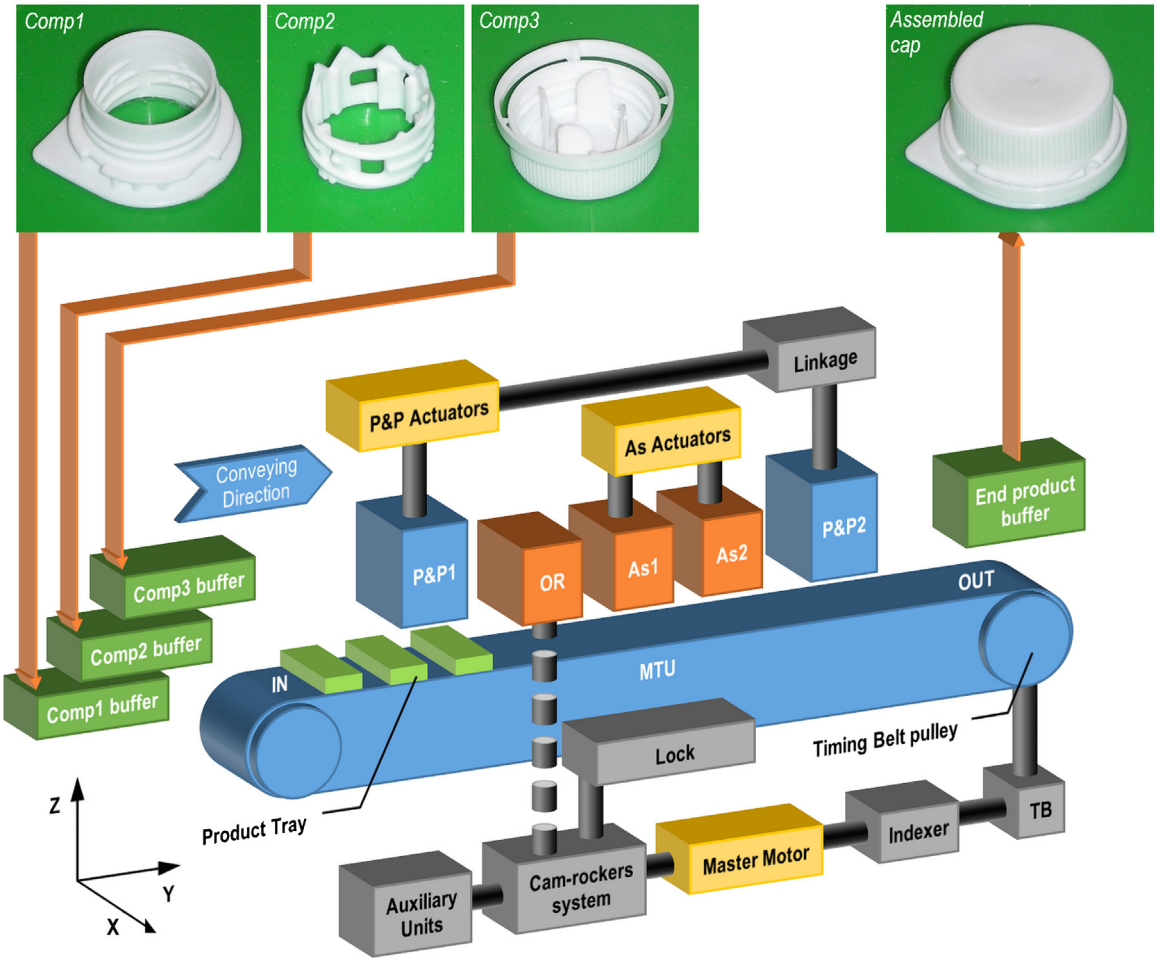

Fig. 1. Simplified schematic of the machine layout.

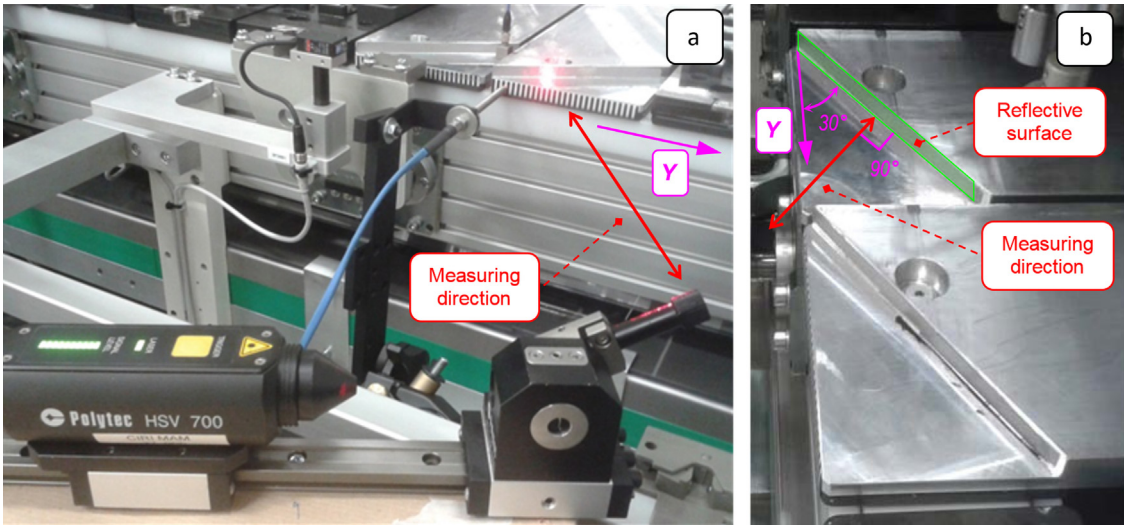

Fig. 2. (a) Laser vibrometer setup and (b) close up of the dummy trays.

laser beam (Fig. 2b). The dummy trays have the same mass and inertia of the regular trays, but they are not suitable for carrying the *Comps*.

An incremental rotary encoder measured both the angular displacement and velocity of the *TB* pulley (Fig. 1). A further encoder monitored the camshaft driving the *OR*.

Piezoelectric accelerometers detected the vibrations of the machine frame and the remaining moving parts (namely *P&P1*,*P&P2*, *As1*, *As2*, *OR*, *Linkage* and *Cam-rockers system*).

All acquisitions were performed by using a LMS SCADAS Mobile SCM-05 system. The "Cycle master phase" signal generated by the machine control unit was also recorded, to be used as an angular reference to synchronize the measured signals with the machine operational phases (one working cycle corresponding to 360°).

The experiments analyzed operation at constant velocity, for different speed values (starting from the nominal value of 680 *ppm* with increments of 40 ppm). Two different machine configurations were tested, referred to as conditions *P1* and *P0* respectively. The former condition featured a fully operative machine, working up to 840 *ppm*. The latter was specifically conceived for both allowing operation up to 1000 *ppm* (thus going far beyond the speed limitation of condition *P1*) and permitting laser vibrometer measurements. In particular, condition *P0* was achieved by modifying condition *P1* as follows. (i) Two product trays were replaced with the dummy trays (Fig. 2b). (ii) The *Lock* unit was deactivated. (iii) The machine ran unloaded, i.e. by removing the *Comps* from the input buffers. In such an instance, the assembly loads normally acting on *As2* were not experienced. Nonetheless, all functional units kept performing their motions, thus inertia actions still affecting the machine operation.

The consistency of the machine behavior in these two configurations was analyzed by the trend of a proper parameter (cfr. Section 4.1).

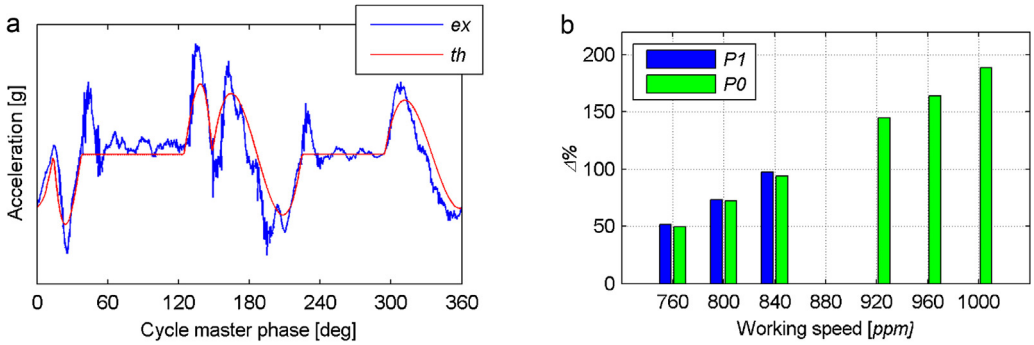

Fig. 3. (a) Experimental (*ex*) and theoretical (*th*) accelerations of the *P&P1* at 1000 *ppm* in condition *P0*, along direction X, over the machine cycle, and (b) index $\Delta\%$ relative to the same transducer for all tested velocities and conditions.

4. Results and discussion

All measurements exhibited very good repeatability over the machine cycle, for all tested conditions. The analysis of the experimental data permitted to identify four functional groups experiencing significant elastodynamic issues, namely the *P&P1*, *OR*, *Linkage* and *MTU*. Results concerning the first three units are discussed in Section 4.1, whereas the fourth unit is examined in Section 4.2.

4.1. Acceleration signals

The accelerations measured on the *P&P1* along the direction *X*, for operation at 1000 *ppm* in condition *P0*, are reported in Fig. 3a (by way of example), as functions of the machine angular reference. The curve describing the corresponding theoretical accelerations (i.e. the law of motion imposed on the *P&P X*-Actuator by the machine controller, which is a known specification of the working cycle) is also shown. Due to a non-disclosure agreement with the machine manufacturer, actual acceleration values cannot be reported whereas only the acceleration profiles can be provided.

For each transducer in each test condition, the root mean square (rms) value of the *residual signal*, i.e. the signal obtained by filtering out the theoretical accelerations from the measured ones, is computed over one machine cycle to globally describe the vibration levels. Then the rms percentage variation (with respect to the nominal functioning velocity, i.e. 680 *ppm*), $\Delta\%$, for the *i-th* acceleration signal is computed as:

$$\Delta\%_{i,Pj,vel} = \frac{rms_{i,Pj,vel} - rms_{i,Pj,nom}}{rms_{i,Pj,nom}} \cdot 100 \tag{1}$$

where *Pj* indicates condition *P1* or *P0*, *nom* refers to the nominal velocity and *vel* is the examined velocity.

Firstly, the trend of such indicator is assessed to confirm the reliability of the tests in the modified condition *P0*. Fig. 3b reports the values of $\Delta\%$ computed in conditions *P1* and *P0* over the tested working speeds for the *P&P1* (direction *X*), presented as an example. The trends of $\Delta\%$ for the two different conditions can be compared up to 840 *ppm*. These results are proven consistent by the comparison (the corresponding rms values being very similar too). A very good match is observed for all the other acceleration signals as well. Hence, the data provided by the tests with modified machine configuration up to 1000 *ppm* can be adopted to confidently predict how the machine would work beyond 840 *ppm* in condition *P1*, i.e. up to the new targeted speed in fully operative configuration.

Secondly, the indicator is exploited to detect abnormal rise in the vibration levels associated with the speed variations. In particular, higher increments in $\Delta\%$ are expected to reveal critical elastodynamic effects. The analysis of the proposed indicator for all acceleration signals identified two critical units, namely the *P&P1* and the *OR*, and confirmed the *Linkage* as potentially troubling, as emerged by visual inspections mentioned in Section 3.

The *P&P1* exhibits values of $\Delta\%$ largely exceeding 150% for both the directions *X* (Fig. 3b) and *Y*, and even over 250% along the Z-axis, at the target velocity of 1000 *ppm* [2]. Such higher vibration levels may lead to the incorrect positioning of the *Comps* in the product trays, thus preventing them from being properly assembled and consequently causing the rejection of all 10 end products on the same tray. The severe vibrations predicted by the investigation may also entail considerable durability issues. Modifying the unit is therefore required. In practice, redesigning the *P&P1* end effector (a rather massive component in the current machine configuration) for reducing its moving inertia appears a feasible strategy for limiting vibration levels.

Severe vibrations characterize also the *OR*, along the *Z*-axis. The comparison between measured and theoretical accelerations along this direction, for operation at 1000 *ppm* in condition *P0*, is shown in Fig. 4a. The corresponding trend of $\Delta\%$ for conditions *P1* and *P0* over the tested working speeds is reported in Fig. 4b. Large oscillations of the *OR* end effector

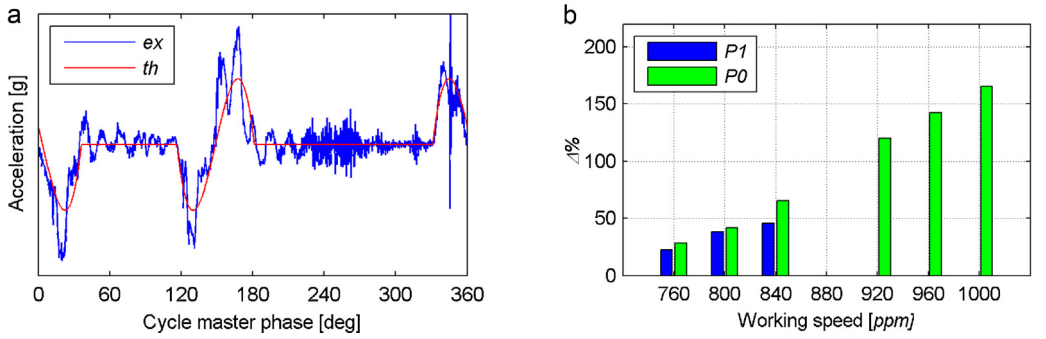

Fig. 4. (a) Experimental (*ex*) and theoretical (*th*) accelerations of the *OR* at 1000 *ppm* in condition *P0*, along direction Z, over the machine cycle, and (b) index $\Delta\%$ relative to the same transducer for all tested velocities and conditions.

may determine incorrect orientation of the *Comps* (and subsequent assembly problems), therefore worsening the machine global performance, similarly to the *P&P1*. In addition, the significant increment in dynamic loads, entailed by vibrations, may raise the failure rate of the *OR* power transmission chain, in particular of its driving cam-rocker system [3]. Reducing the mass of the *OR* end effector is essential for addressing these issues.

The *Linkage* is characterized by remarkable oscillations of its two principal components, namely two long carbon fiber couplers. Analyses in both the frequency and the time domains [2] reveal that operation at 1000 *ppm* triggers the resonances of the couplers up to the third natural frequency. These local elastodynamic phenomena, however, do not prove detrimental for the machine performance, since the *P&P2* keeps working regularly at 1000 *ppm*. Nonetheless, stiffening the *Linkage* for incrementing its natural frequencies and lowering deformations would be advisable in order to avoid possible durability issues.

4.2. Laser vibrometer and encoder signals

Estimating the motion of the product trays at the new target velocity was considered essential, since the preliminary check had suggested that the *MTU* belt conveyor might present excessive compliance. Significant tray oscillations may determine incorrect synchronization with the *Lock* engagement, which would result potentially harmful to the integrity of several machine components. Hence the investigation focuses on the displacement signals, whereas the velocity ones are only used for verification purpose. In particular, the laser vibrometer measurements are analyzed in terms of overshoot and peak-to-peak oscillation with respect to the tray rest position, which is theoretically reached at the end of the *MTU* active phase (lasting 120° of the machine cycle), after a displacement of 120 mm.

Fig. 5a reports the overshoot and peak-to-peak oscillation of the tray displacement for some tested velocities in condition *P0*. Neither quantity exhibits a monotonic growth with the increasing speed. Reasonably, some kind of antiresonant effect is present around 920 *ppm*, whereas operation at the highest velocities triggers one of the system natural frequencies (at about 14 Hz). Indeed large tray oscillations occur at 1000 *ppm*, which are not compatible with the correct machine functioning.

The vibrometer measurements and the data provided by the encoder monitoring the *TB* pulley are compared to find the source of the observed elastodynamic effects. The peripheral displacement of the toothed pulley is computed from the encoder signals by considering a pitch radius of about 114.6 mm (the pulley having 36 teeth and a 20 mm pitch). As an example, Fig. 5b shows a close up of the tray displacement and the *TB* pulley peripheral displacement around 120° of the cycle master phase, at 1000 *ppm*. The comparison clearly reveals that the tray displacement is almost completely ascribable to the *TB* compliance, whereas, contrary to initial assumptions, deformations occurring in the *MTU* belt conveyor are rather negligible (the tray on the *MTU* basically follows the *TB* pulley peripheral displacement). The same conclusion can be drawn for all tested velocities.

A new close inspection of the *TB* inside the machine detected the presence of extremely large belt deformations. Such deformations may cause the belt to jump teeth, thus leading to loss of synchronism between the *MTU* and the machine phase, and consequently to a critical failure. Furthermore, the excessive tray overshoot would rapidly damage the *Lock* and other auxiliary units. Reducing the *MTU* inertia and increasing the *TB* stiffness are both required for limiting oscillations.

In practice, the former strategy may be carried out by decreasing the mass of the product trays. The latter may be implemented by increasing the radius of both *TB* pulleys, as the belt equivalent torsional stiffness reduced to the *j-th* axis, K_{Tj}, is given by [4]:

$$K_{Tj} = 2K_B r_j^2 \quad ; \quad K_B = c_{sp}\frac{b}{L_i} \tag{2}$$

being K_B the belt stiffness, r_j the pitch pulley radius, c_{sp} the specific belt stiffness (provided by the manufacturer), b the belt width and L_i the belt free span.

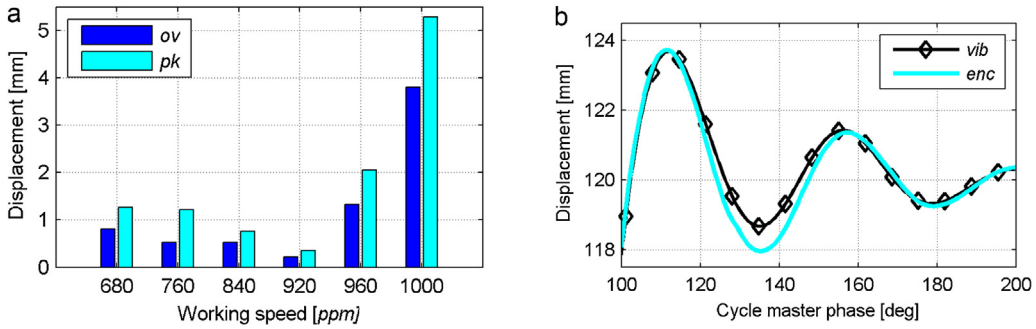

Fig. 5. (a) Overshoot (*ov*) and peak-to-peak (*pk*) oscillation of the tray displacement as functions of the working speed; (b) comparison between tray displacement (*vib*) and pulley peripheral displacement (*enc*) at 1000 *ppm*.

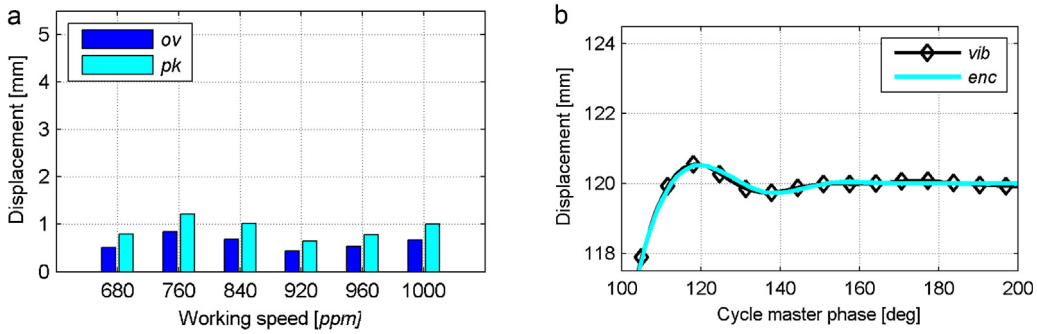

Fig. 6. Experimental results after *MTU* partial redesign: (a) overshoot (*ov*) and peak-to-peak (*pk*) oscillation of the tray displacements as functions of the working speed; (b) comparison between tray displacement (*vib*) and pulley peripheral displacement (*enc*) at 1000 *ppm*.

A variant of the original machine was arranged and tested. It was obtained by implementing just one modification of the previous design, namely by replacing all the product trays of the *MTU* with lighter new ones. In particular, each product tray was redesigned by cutting down its mass by about 33%, thus significantly reducing the *MTU* total inertia. Indeed the original trays were found to be considerably oversized with respect to the minimum structural strength requirements.

The tray displacements measured in these additional experiments are reported in Fig. 6. In particular Fig. 6a shows the overshoot and peak-to-peak values for all tested velocities, whereas the comparison between the tray displacement and the *TB* pulley peripheral displacement at 1000 *ppm* is reported in Fig. 6b. Vibrations appear significantly reduced. Therefore this single design modification is proven effective for mitigating the elastodynamic issues affecting the *MTU*.

It is worth noting, however, that implementing also the other proposed modifications (in particular those concerning the *P&P1* and *OR*, as reported in Section 4.1) still appears advisable in order to achieve a satisfactory working performance of the machine when operating with the new desired production capacity.

5. Conclusions

This paper reported the experimental investigation, by means of vibration measurements, of the elastodynamic phenomena affecting an automatic machine for plastic cap assembly when exceeding the nominal working speed by 50%, that is a new requirement to raise the machine production capacity.

The special machine reconfiguration and test conditions adopted for the experiments permitted to reliably predict the machine response at the new targeted working speed. The analysis successfully identified the most troubling functional units, and allowed the development of proper strategies to solve the critical issues. Further tests performed after implementing the partial redesign of the most critical unit showed a remarkable reduction of vibration levels and elastodynamic phenomena, thus proving the effectiveness of the proposed solutions.

References

[1] C. Miani, D. Veroni, C. Casale. Closable opening device for sealed packages of pourable food products. European Patent Application 1262412A1, 2002.
[2] A. Martini, M. Troncossi, Analysis and prediction of the elastodynamic behavior of an automatic machine for plastic cap assembly by means of vibration measurements, Proc. of the XXII Conference of the Italian Association of Theoretical and Applied Mechanics (AIMETA 2015), Genova, Italy, September 14–17, 2015, pp. 170–179. ISBN 978-88-97752-55-4 (accessed 03/14/2016) http://www.aimeta2015.dicam.unibo.it/node/23.
[3] A. Martini, M. Troncossi, A. Rivola, Experimental vibration analysis of an automatic machine for plastic cap assembly, Proc. of the 8th International Conference on Acoustical and Vibratory Surveillance Methods and Diagnostic Techniques (Surveillance 8), Roanne, France, October 20–21, 2015, pp. 1–8.
[4] M. Ebrahimi, R. Whalley, Analysis, modeling and simulation of stiffness in machine tool drives, Comput. Ind. Eng. 38 (1) (2000) 93–105.